YIG magnonics

2010 J. Phys. D: Appl. Phys. 43 264002

(http://iopscience.iop.org/0022-3727/43/26/264002)

IOP PUBLISHING JOURNAL OF PHYSICS D: APPLIED PHYSICS

J. Phys. D: Appl. Phys. **43** (2010) 264002 (16pp) doi:10.1088/0022-3727/43/26/264002

YIG magnonics

A A Serga, A V Chumak and B Hillebrands

Fachbereich Physik and Forschungszentrum OPTIMAS, Technische Universität Kaiserslautern, 67663 Kaiserslautern, Germany

E-mail: hilleb@physik.uni-kl.de

Received 7 April 2010, in final form 29 April 2010
Published 17 June 2010
Online at stacks.iop.org/JPhysD/43/264002

Abstract

Early experiments in magnonics were made using ferrite samples, largely due to the intrinsically low magnetic (spin-wave) damping in these materials. Historically, magnonic phenomena were studied on micrometre to millimetre length scales. Today, the principal challenge in applied magnonics is to create sub-micrometre devices using modern polycrystalline magnetic alloys. However, until certain technical obstacles are overcome in these materials, ferrites—in particular yttrium iron garnet (YIG)—remain a valuable source of insight. At a time when interest in magnonic systems is particularly strong, it is both useful and timely to review the main scientific results of YIG magnonics of the last two decades, and to discuss the transferability of the concepts and ideas learned in ferrite materials to modern nano-scale systems.

(Some figures in this article are in colour only in the electronic version)

1. Introduction

In this review we address the field of spin waves in magnetic films and nanostructures [1–4], nowadays called 'magnonics' [5, 6]. This field encompasses the transmission, storage and processing of information using packets of spin waves. Spin waves—or magnons, the quanta of spin waves—represent eigenexcitations of the electron spin subsystem in magnetically ordered media and are observed in ferro- and ferrimagnets, as well as in antiferromagnets. The interaction between nuclear and electronic spins at low temperatures can also lead to the appearance of nuclear spin waves [7]. This special class of spin waves constitutes an important field of research in its own right and does not form part of our review [8–10]. Electronic spin waves have attracted significant interest since the beginning of the 20th century, both for their interesting underlying fundamental physics and for their potential technological applications. Perhaps more than any other kind of wave (for example electromagnetic or acoustic), spin waves display a diversity of dispersion characteristics. These can be varied via a wide range of parameters, including the choice of magnetic material, the shape of the sample and the orientation and size of applied bias magnetic field. The combination of a rich choice of linear spin-wave properties and strongly pronounced nonlinear effects make spin-wave systems an interesting environment for the study of general wave dynamics. One- and two-dimensional soliton formation, different types of parametric instability, wavefront reversal processes, self-oscillating systems and room temperature Bose–Einstein condensation of magnons, are just a small selection of the effects which have already been subjected to intensive study.

Spin waves typically exist in the microwave frequency range and their wavelength can be decreased to the nanoscale, making them a promising prospect for the development of microwave information processing devices. Research in this area was at its height between 1960 and 1980, inspired—at least in part—by the discovery of a new material: yttrium iron garnet (YIG) with uniquely low magnetic damping. A wide range of innovative YIG-based devices for analogue signal processing were developed over this period, but many have since been displaced by new technologies. In particular, few have been able to survive competition from semiconductor devices.

However, recent years have seen a resurgence of interest in spin waves within the scientific community, motivated by their possible use as information carriers in spintronic applications. Information in spintronic systems is encoded on electron spins, rather than charges as in conventional electronics. Potentially, spins can be manipulated without current, overcoming an important fundamental limitation of conventional electronics: a power consumption which scales linearly with increasing number of individual processing elements. This technological opportunity lends new momentum to the study of fundamental

spin-wave properties. Spin waves can be studied in a range of materials. From a practical point of view, perhaps the most attractive are polycrystalline magnetic metals and alloys, which are well suited to nano-fabrication techniques. However, very large intrinsic spin-wave damping in such materials (which normally does not allow propagation to be observed over distances more than a few tens of micrometres), as well as technical problems associated with spin-wave excitation and reception make these materials a challenging experimental environment. Until materials advances provide solutions to these issues, continued study of spin waves in YIG is highly profitable. Fundamental insight into spin-wave dynamics gained in YIG—in which it is possible to capitalize on the convenience of low damping—is readily transferable to other material systems. At the same time, this transfer can be performed only after careful consideration and comprehensive analysis of the specificities of a micro-scaled system, as highlighted for example by the recently observed influence of internal magnetic field inhomogeneity and high damping on linear and nonlinear spin-wave dynamics in metallic waveguides and rings [11–14].

In this paper we address the main achievements in YIG-based spin-wave dynamics over the last two decades. An attempt is made to cover both the study of the pure physics of linear and nonlinear spin-wave dynamics and of multi-interactions of quasi-particles, and the application-oriented study of spin-wave properties.

In section 1 we give a short overview of the structure and properties of yttrium iron garnet (YIG), spin wave characteristics in thin films and common experimental techniques. This introductory section essentially provides a summary of several excellent review papers and books which have tackled various aspects of the subject before.

In the main text of the paper we highlight key experimental results in fundamental and applied spin-wave studies. Given the huge volume of work which has been performed over the time period covered by the review, it is inevitable that there are some omissions, and we offer our apologies to the author of any study which appears to have been overlooked. We stress that this is not because we consider the work unimportant, but simply because lack of space forces us to place some limitation on scope.

In accordance with the definition of the term 'magnonics' given above, we focus on topics connected with the processing of information using spin-wave systems, most particularly spin-wave packet propagation in nonuniform media and magnonic crystals, parametric amplification and wavefront reversal processes, and signal storage and recovery phenomena in multi-mode spin-wave systems.

In the final section we summarize the results described and discuss their importance and wider context.

2. General overview

In this section we offer some basic information which will be useful to the nonspecialist reader in understanding the themes tackled in the rest of the paper. We discuss the material YIG, the types of spin waves which can be excited in thin-film waveguides and the experimental techniques commonly employed in their study. We refer the specialist reader in search of more detailed information or insight to a range of excellent references.

2.1. Structure and main properties of yttrium iron garnet (YIG)

One of the most significant challenges in the study and technological application of spin waves is that the relaxation parameters associated with typical experimental spin-wave systems are large. The magnon lifetime in pure iron and in the commonly used polycrystalline alloy permalloy ($Ni_{81}Fe_{19}$) is of the order of nanoseconds [15, 16]. Short lifetimes together with slow magnon speeds (approximately four orders of magnitude slower than the speed of light) combine to produce spin-wave mean free paths typically less than 10 μm [17, 18].

King among low-damping magnetic materials is monocrystalline yttrium iron garnet $Y_3Fe_5O_{12}$ (YIG) [19, 20, 21]. This ferrimagnet has the narrowest known line of ferromagnetic resonance (FMR)—generally smaller than 0.5 Oe—which results in a magnon lifetime of a few hundred nanoseconds. Low damping in YIG allows spin-wave propagation to be observed over centimetre distances. Moreover, nonlinear dynamic effects are strongly pronounced in YIG [22–26]. As a result, this material finds widespread use in microwave devices (including high-Q microwave oscillators, generators, filters and power limiters) [21, 26–28], and it is an excellent material for the study of linear and nonlinear spin-wave dynamics [22, 24, 25]. YIG also attracts attention as a result of a high magneto-optical efficiency [29–32], but a discussion of this area is beyond the scope of this paper.

Yttrium iron garnet has a complicated cubic crystal structure. Each unit cell of dimension 12.376 Å houses 80 atoms, with twenty magnetic Fe^{3+} ions being distributed over two antiferromagnetically coupled octahedral (8 ions) and tetrahedral (12 ions) sub-lattices. The crystallographic properties have been studied in detail [19–21], as have the optimal conditions for YIG fabrication [33, 34].

The production of high-quality, thin-film YIG spin-wave waveguides opened up new possibilities for the study of spin waves and spin-wave dynamics. The best thin films obtained to date have been grown by high-temperature liquid phase epitaxy on gallium gadolinium garnet (GGG) substrates [35–37]. The lattice constant of GGG (12.383 Å) is very well matched to YIG, enabling the fabrication of high quality, defect-free unstressed films. However, the best matching is achieved by light doping of YIG by lanthanum or gallium [37]. Careful optimization of the growth technique results in high purity films with an FMR linewidth as narrow as that of bulk YIG. Most of the results presented in this paper have been obtained using YIG films grown in this way with a surface normal parallel to the $\langle 1\,1\,1\rangle$ crystallographic axis. YIG thin films in widespread academic use typically have a saturation magnetization $4\pi M_0 = 1750$ G, and exchange constant $\alpha = q/(4\pi) = 3 \times 10^{-12}$ cm^2.

As well as attracting interest in a fundamental research context, the availability of low-damping YIG waveguides

also led to the development of many spin-wave based analogue signal processing devices. Among the linear spin-wave based devices which have been reported are delay lines, filters, resonators, generators, pulse separators, multi-channel receivers, compressive receivers, directional couplers and Y-circulators. Noteworthy devices based on nonlinear spin-wave properties include frequency-selective power limiters, signal-to-noise enhancers, parametric amplifiers and convolvers. The most important achievements in this area are discussed in several review papers (for example by Adam [38] and Ishak [39]).

2.2. *Spin wave characteristics in thin films*

This section is devoted to a short overview of the main types of spin waves in thin-film waveguides. We will not consider spin waves and oscillations in bulk samples, concentrating solely on so-called magnetostatic spin waves (MSWs) [40–42].

For the uninitiated, the term magnetostatic spin waves can be a little unhelpful, since it seems to call into question the waves' status as 'dynamic phenomena'. It is important to stress that the word magnetostatic is used here simply to indicate that the waves represent solutions to Maxwell's equations with a magnetostatic approximation, which assumes negligible displacement current and a spin-wave wavelength significantly shorter than that of an electromagnetic wave of the same frequency. Despite the fact that the legitimacy of the magnetostatic approximation improves as the spin-wave wavelength decreases, for historical reasons, a lower limit is placed on the MSW wavelength. This limit signifies the point at which the exchange interaction, which is not modelled by Maxwell's equations, begins to strongly influence wave properties. The exchange interaction is highly sensitive to the relative orientation of neighbouring spins, and thus has negligible influence at long wavelengths. Typical MSW wavelengths lie in the micrometre to millimetre range. MSW wave frequencies in YIG are primarily determined by the value of the applied bias field, and are generally between 1 and 40 GHz [40–42].

Three distinct classes (often termed modes) of MSW can be excited and propagate in a thin magnetic waveguide. In a given structure, the class of spin-wave excitation is determined by the orientation of the applied bias magnetic field relative to the direction of spin-wave propagation. The three classes are distinguished by markedly different dispersion properties (i.e. $f(k)$ relations) and are generally studied independently. The classic work in this area was performed by Damon and Eschbach [40–42]. Since then, many excellent books have been written on the subject (for example [24–26, 43–45]).

Forward volume magnetostatic spin waves (FVMSWs) are associated with a magnetic waveguide magnetized normally to its surface [42], perpendicular to the direction of spin-wave propagation. The dispersion curve for FVMSW is shown in figure 1(*a*). The spin-wave frequency as the wavenumber k tends to zero, tends to the value $f_H = \gamma H_0$, where H_0 is the effective internal field (with the geometrically dependent demagnetizing field taken into account) and $\gamma = 2.8\,\mathrm{MHz\,Oe^{-1}}$, the electron gyromagnetic ratio. With increasing k, the spin-wave frequency tends to $f_1 = \sqrt{f_H(f_H + f_M)}$, where $f_M = 4\pi\gamma M_0$ and M_0 is the saturation magnetization. The slope of the curve is determined mostly by the film thickness. An important and distinguishing feature of FVMSW is the invariance of their dispersion with direction of propagation in the plane of the film, which can easily be understood from the fact that the waves always propagate normally to the bias field. A useful approximation to the FVMSW dispersion relation is given by [43, 46]

$$f_{\mathrm{FVMSW}} = \sqrt{f_H\left(f_H + f_M\left(1 - \frac{1 - \exp(-kd_0)}{kd_0}\right)\right)}. \qquad (1)$$

This expression is used to calculate the curve of figure 1(*a*).

Two different MSW mode-types can be excited in a thin-film waveguide magnetized in-plane [41]: backward volume magnetostatic waves (BVMSW), associated with propagation direction parallel to the applied bias field, and magnetostatic surface spin waves (MSSW) which occur when the bias field is perpendicular to the propagation direction.

The dispersion curve for BVMSWs is shown in figure 1(*b*) and can be approximated by [43, 46]

$$f_{\mathrm{BVMSW}} = \sqrt{f_H\left(f_H + f_M\frac{1 - \exp(-kd_0)}{kd_0}\right)}. \qquad (2)$$

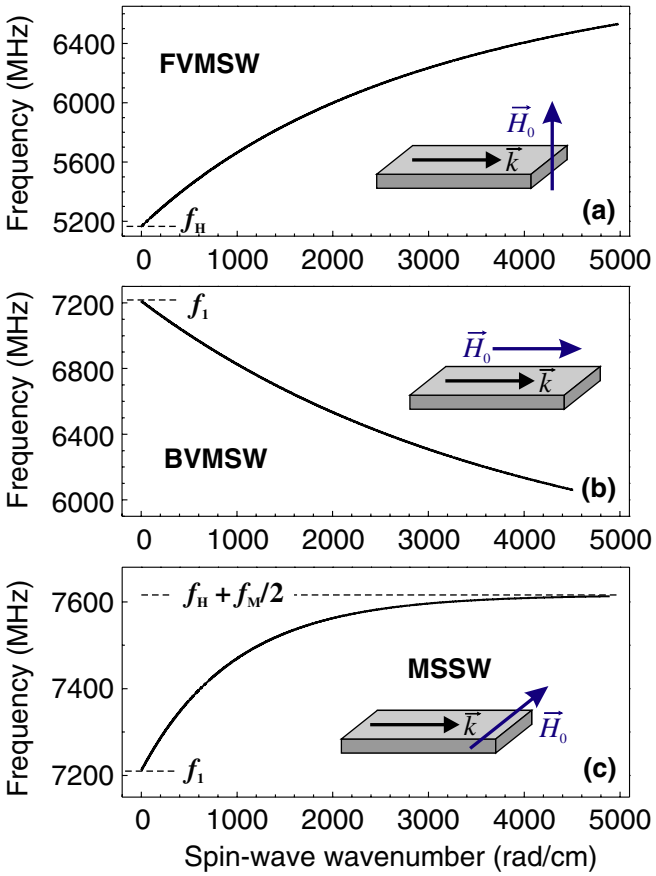

Figure 1. Calculated dispersion characteristics using formulae (1), (2) and (3) for (*a*) forward volume magnetostatic waves, (*b*) backward volume magnetostatic waves, (*c*) magnetostatic surface spin waves. Bias magnetic field $H_0 = 1845$ Oe, saturation magnetization $4\pi M_0 = 1750$ G, film thickness $d_0 = 5\,\mu$m. (Lowest order thickness modes shown.)

The curve has the appearance of a mirrored version of the FVMSW characteristic: spanning the region between f_1 and f_H. Like FVMSW, BVMSWs are volume modes. This means that the amplitude of the magnetization precession has a cosinusoidal distribution across the film thickness. The main peculiarity of BVMSW is the negative slope of their dispersion curve, and consequently the negative group velocity $v_{gr} = \partial f/\partial k$. This unusual physics implies that the phase and group velocities of the waves are counter-propagating and an increase in k is associated with a decrease in wave frequency.

Unlike backward and forward volume waves, magnetostatic surface spin waves (MSSWs) are localized to one surface of the film in which they propagate. The distribution of precessional amplitude across the film thickness is exponential, with a maximum at one surface of the film. For the particular orientation of bias magnetic field and the MSSW propagation direction shown in figure 1(*c*) this maximum is located on the upper film surface; it can be switched to the lower surface by reversal (i.e. a 180° rotation) of either the field or the propagation direction. The dispersion curve for MSSW is shown in figure 1(*c*), calculated using the formula [43, 47]

$$f_{MSSW} = \sqrt{(f_H + f_M/2)^2 - (f_M/2)^2 \exp(-2kd_0)}. \quad (3)$$

In the small wavenumber limit, the spin-wave frequency is the same as that of BVMSW and is equal to f_1, the ferromagnetic resonance frequency (FMR) for the film magnetized in-plane. With increasing k, the MSSW frequency tends to the value $f_H + f_M/2$ [41].

It should be noted that in figure 1, the dispersion relationships are shown for the lowest (uniform) thickness modes. Higher-order thickness modes having nonuniform amplitude distribution across the film thickness are described by other dispersion laws [41, 43, 44], but are not so important for this review since they generally have lower excitation efficiencies. All three classes of waves may be excited in a thin-film waveguide using a microstrip antenna. For this type of excitation, MSSWs have the highest excitation efficiency, but they are also nonreciprocal (see [48] and references therein). This means that a microstrip excites a wave which propagates in a unique direction along the film. It should be appreciated that this nonreciprocity in *excitation* does not originate from the nonreciprocal surface *localization* of the MSSW amplitude maximum discussed above. In most practical experimental systems, the film thickness is significantly smaller than the MSSW wavelength ($kd_0 \ll 1$) and the distribution of the wave amplitude across the film thickness is thus approximately uniform [49]. Nonreciprocal excitation is owed to the interference of waves excited by the in- and out-of-plane components of the microwave magnetic field produced by the microstrip antenna, which is constructive for one propagation direction and destructive for the other.

Early spin-wave studies were focused mainly on MSSW and FVMSW modes. This was largely—if not exclusively—for practical reasons. It is technically much more straightforward to realize homogeneous bias magnetic fields oriented in the out-of-plane and transverse directions relative to a long, thin-film section, compared with along its axis. However, over the last decade, as experimental techniques have matured, interest in BVMSW has grown significantly. As well as being the most technically demanding, BVMSWs are in many ways the most interesting class of spin waves to study, owing to their unique dispersion characteristics, and particular nonlinear properties. Latterly, attention has also been drawn to short wavelength spin waves with properties influenced not only by the dipolar interaction but also by exchange. These waves, termed dipole-exchange spin waves (DESW), have been the subject of several detailed studies [46, 47].

2.3. Techniques commonly employed in the experimental study of spin waves

This section describes some of the main techniques employed in the experimental study of spin-wave systems. In particular, we outline standard methods of spin-wave excitation and detection. An appreciation of these techniques should aid understanding of the results discussed in the rest of the paper.

We will first explore the topic of spin-wave excitation and detection by means of simple microstrip microwave antennas. Figure 2(*a*) shows a YIG waveguide with two microstrip antennas: an input and an output. In a typical experiment, the waveguide might have a width of 2–3 mm, a length of several centimetres and a thickness between 1 and 10 μm. It is standard practice to cut the edges of the waveguide at a 45° angle in order to avoid spin-wave reflection. As discussed in the previous section, the class of spin-wave which is excited and propagates in such a waveguide is determined by the orientation of the applied bias field relative to the propagation direction. The strength of the field is chosen to be sufficient to assure full magnetic saturation.

Figures 2(*a*) and (*b*) correspond to the BVMSW geometry. In order to understand the spin-wave signal excitation and reception mechanism, it is useful to consider the waveguide as a reservoir of quasi-classical spins. When the waveguide is magnetically saturated, the mean precessional axis of all the spins is parallel to the bias field. Application of a microwave signal to the input antenna generates an alternating Oersted magnetic field as indicated in the inset to figure 2(*a*). The horizontal component of this field is oriented along the bias direction, and thus cannot exert a torque on the spins. The vertical component is perpendicular to the mean precessional axis and creates a torque which results in an increase in precessional amplitude above the thermal level. Spins which precess under the antenna interact with their nearest neighbours and—when proper conditions of field and frequency are satisfied—spin-wave propagation is supported. The mechanism of spin-wave detection is—by symmetry—the inverse of the excitation process, when the spin-wave arrives, it induces an ac current in the output antenna.

The simple passive delay line of figure 2(*a*) can be used to gather interesting insight into spin-wave phenomena. Applying a variable-power continuous wave or pulsed signal to the input antenna and connecting an oscilloscope to the output allows the linear and nonlinear dispersion characteristics of the waveguide to be studied. Connecting a network analyzer to the

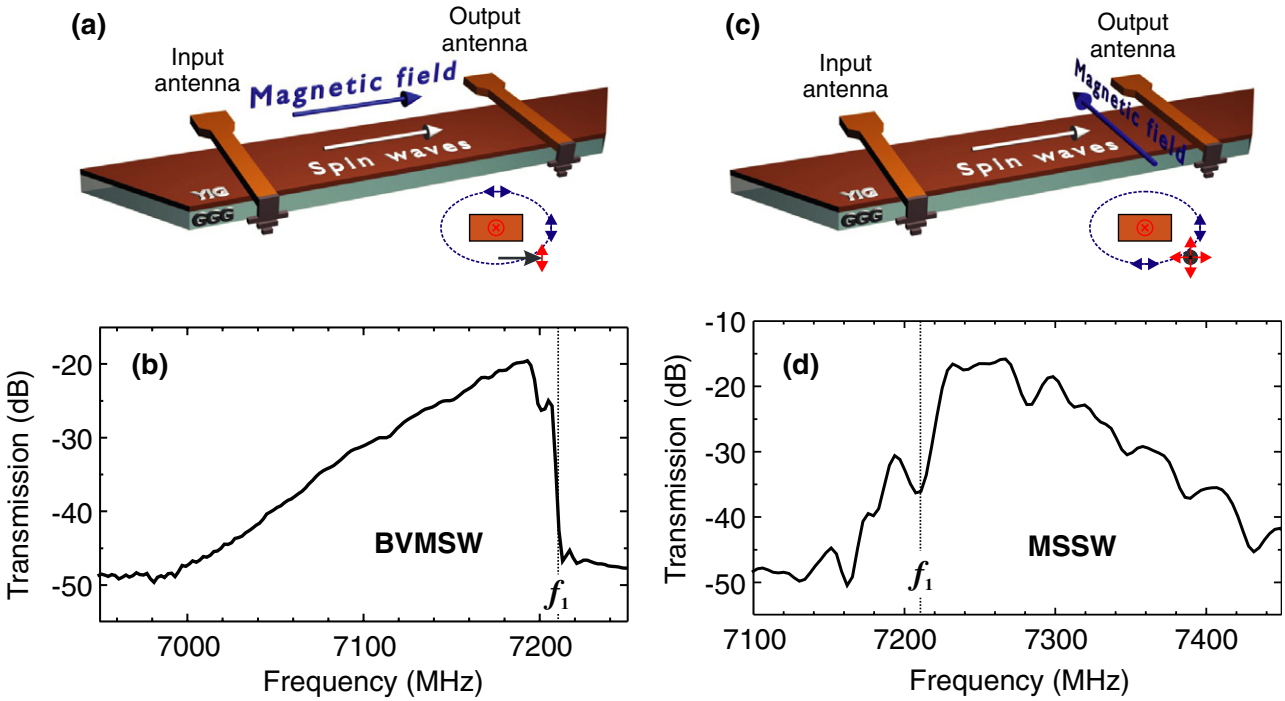

Figure 2. Sketch of BVMSW (*a*) and MSSW (*c*) experimental setups. Insets schematically illustrate the excitation mechanism. Typical transmission characteristics (S_{21}) for BVMSW (*b*) and MSSW (*d*) waves. Bias magnetic field $H_0 = 1845$ Oe, film thickness $d_0 = 5\,\mu$m, the antenna separation is 8 mm.

structure and obtaining *S*-parameter data (i.e. the reflection parameters S_{11} and S_{22} from the antennas, and the forward and reverse transmission parameters S_{21} and S_{12}) can also be extremely informative.

Simple microwave signal processing can even be achieved in such a system; however, losses—which are jointly determined by the efficiency of the spin-wave excitation and the detection mechanism, and dissipation in the waveguide—are typically large, and can exceed 20 dB.

Figure 2(*b*) shows a typical transmission characteristic (S_{21}) for BVMSW. The bias magnetic field corresponds to that for the calculation shown in figure 1(*b*). The high-frequency limit on spin-wave excitation is the FMR frequency f_1. The maximum of the transmitted signal corresponds to spin waves in the limit $k \to 0$. With decreasing BVMSW frequency (increasing wavenumber) the intensity of the transmitted signal decreases. This is explained by a decrease in the excitation and detection efficiencies of the antennas at short wavelengths. Generally, the width of the antennas places a lower limit on the wavelength of spin-wave excitation. The level outside of the transmission band (around −50 dB in figure 2(*b*)) is determined by direct electromagnetic leakage between the antennas.

An experimental arrangement for the study of MSSW is shown in figure 2(*c*). It differs from the BVMSW setup only by the orientation of the bias magnetic field. However, as indicated in the inset figure, the geometry of the excitation mechanism leads to pronounced differences in behaviour. Here, not one but two components of the microwave signal applied to the antenna—vertical and horizontal—participate in spin-wave excitation. This results in an increase in the excitation efficiency (compare figures 2(*b*) and (*d*)) and also leads to nonreciprocity. When the antenna is excited with a microwave signal, the resulting spin-wave propagates only in one direction (i.e. to the left or right of the antenna) and is localized to a single surface (although as discussed in section 2.2, in most practical experimental systems, the film thickness is significantly smaller than the MSSW wavelength ($kd_0 \ll 1$) and the distribution of the wave amplitude across the film thickness is effectively uniform, see [48] and references therein). Figure 2(*d*) shows an experimental MSSW transmission characteristic, in agreement with the calculated dispersion relation of figure 1(*c*), the lower frequency limit f_1 corresponds to the FMR frequency. The efficiency of the excitation is again highest for small wavenumbers. The small gaps in the transmission curve occur as a result of crossings of the MSSW dispersion curve with standing thickness DESW modes at frequencies above f_1 [47].

Apart from pure microwave studies, a detection technique used extensively in spin-wave research is Brillouin light scattering (BLS) spectroscopy [32]. The physical basis of BLS spectroscopy is inelastic scatter of photons by magnons. Scattered light from a probe beam, incident on the sample is analysed. Determination of the scattered (Stokes and anti-Stokes) photon frequencies and wavenumbers allows the frequencies and wavenumbers of the scattering magnons to be determined, and the scattered photon intensity is proportional to that of the spin wave. The technique is generally used in conjunction with a microwave excitation scheme and—over the last decade—has undergone extensive development. BLS spectroscopy now achieves a spatial resolution of 250 nm [50] and time- and phase-resolved systems [51, 52] have recently yielded several important results [48, 53].

3. Spin-wave propagation in nonuniform media and magnonic crystals (MCs)

In this section we consider linear spin-wave behaviour in nonuniform media. Two main topics are discussed: spin-wave propagation through waveguides with nonuniform dispersion properties, and spin-wave reflection and tunnelling from areas or regions of waveguide where spin-wave propagation is entirely disallowed. We also review the subject of magnonic crystals: periodic magnetic meso-crystals with special dispersion characteristics.

3.1. Spin-wave propagation through a single localized inhomogeneous magnetic region

Propagation of spin waves in nonuniform magnetic fields was first discussed in the 1960s [54, 55]. In this first section, we focus on spin-wave propagation through individual, localized magnetic inhomogeneities. This class of system offers insight into almost all of the most important relevant aspects of spin-wave behaviour, and provides the basis for theoretical and experimental studies of more complicated structures.

In order to analyse the behaviour of spin waves in the region of a localized magnetic inhomogeneity, it is necessary to distinguish between two classes of system: those in which the inhomogeneity takes the form of a single localized area where the spin-wave dispersion characteristics differ from the bulk, and those in which the inhomogeneity is such that spin-wave propagation is not merely altered, but entirely prohibited. Spin-wave scattering and energy transfer mechanisms differ significantly in the two cases. For the first, the defining parameters are the relative fractions of stored and reflected wave energy at the interface between the region and the inhomogeneity. In the second case, spin-wave tunnelling effects dominate. It was Schlömann who first noted a close parallel between propagation of exchange-dominated spin waves in the region of a magnetic inhomogeneity and the motion of a quantum-mechanical particle in a potential well [55]. In order to reap the benefits of such a useful analogy, it is necessary to consider how to determine spin-wave tunnelling energies and probabilities and—importantly—what magnetic energy contribution (dipolar or exchange) plays the dominant role.

Many different methods of creating a magnetic inhomogeneity in a spin-wave waveguide have been demonstrated. One possibility is to alter the effective external magnetic bias in a localized region [56–58]. This can be achieved via the Oersted field from a direct-current-carrying wire, placed in contact with the surface of a YIG waveguide. In order to perform an experiment using such a system, it is necessary to choose the correct orientation of the wire relative to the spin-wave propagation direction and bias field. For MSSW and FVMSW this is problematic, but for BVMSW the situation is straightforward: it is sufficient to simply place the wire on top of the waveguide perpendicular to the propagation axis.

The spatial extent and the strength of the inhomogeneity are determined primarily by the value of the applied current. By tuning the value of the bias field it is possible to shift the dispersion curve (figure 1(*b*)) in such a way that—for constant spin-wave frequency—the spin-wave wavenumber can be varied, or the conditions for spin-wave exclusion created (spin-wave frequency f_s larger than the FMR frequency $f_s > f_1$).

Results of a detailed experimental study into tunnelling of dipole-dominated BVMSW through inhomogeneities created by current-carrying wires have established that either a barrier or a well for spin-wave transmission can be created, each corresponding to a given polarity of current (and therefore Oersted field). The current dependence of the amplitude of spin-wave transmission through a spin-wave well is non-monotonic with a single minimum and two maxima. One maximum represents the low current limit whilst the second is a scattering resonance [57].

Spin-wave tunnelling through magnetic barriers has recently been the subject of extensive study [56]. It has been established that the magnetic dipole interaction plays a dominant role in determining tunnelling parameters. Additionally, it has been shown both experimentally and theoretically that because the character of the magnetic dipole interaction is nonlocal, the tunnelling transmission coefficient depends nonexponentially on the barrier width.

As well as being dependent on the magnitude and polarity of the applied field disturbance, spin-wave reflection from a magnetic inhomogeneity varies with the spin-wave frequency. For an inhomogeneity in the form of a localized region of decreased magnetic bias (the tunnelling regime) there is a monotonic relationship between the wave frequency and the reflection efficiency. However, in the opposite case (the so-called diffractive regime) a resonant behaviour is observed, and reflection is pronounced only over a small frequency range below the FMR [58].

Spin-wave transmission in the tunnelling regime can be much higher than in the diffractive regime (as much as 25 times). Moreover, the formation of a soliton—a nonlinear spin-wave packet—can result in either enhancement or suppression of the reflection efficiency, depending on whether the system is tunnelling or diffractive in character [59].

The phenomenon of resonant spin-wave tunnelling in a twin-barrier system has also been reported. Here, the single current-carrying wire of the experiments described above is replaced by two identical parallel wires in close proximity. For a certain spin-wave wavelength (dependent on the inter-wire distance) resonant tunnelling is observed and spin-wave transmission through the double-barrier structure is enhanced with respect to that for two identical independent barriers [60].

Another means of forming a localized barrier to spin-wave propagation is to fabricate a mechanical gap in a waveguide [61]. In such a system, tunnelling efficiency is primarily determined by the gap width, an increase in the gap width (or the spin-wave wavenumber at fixed gap width) leading to a reduced transmission. The gap width-transmission dependences can be reconciled with the characteristics of the dynamic dipolar field formed by the incident spin wave. Comparisons with theoretical calculations show that an additional demagnetization field due to the gap has a significant impact on the transmission, leading to an effective increase in the width.

3.2. Current-controlled magnetic mirrors and spin-wave logic

In the previous section, we discussed the transmission of dipole-dominated spin waves through localized static magnetic inhomogeneities. Dynamic magnetic inhomogeneities—formed for example by applying alternating or pulsed currents to surface current-carrying conductors—allow yet further interesting effects to be observed.

An experiment which illustrates the key concepts in this area particularly well is based on the use of two closely spaced current-carrying wires arranged on a YIG waveguide between a set of conventional microstrip antennas (input and output) [62]. Initially, a direct current is applied to the furthest wire only. A short spin-wave pulse is excited at the input antenna which propagates to this structure and is reflected. Before the reflected pulse reaches the vicinity of the first wire, this too is supplied with current and—as a result—the excitation is trapped and forced to oscillate between a set of 'magnetic mirrors'. By tuning the reflectivity of the mirror system via the amplitudes of the applied currents, it is possible to allow a measurable fraction (for example one tenth) of the spin-wave energy to pass through at each reflection event, permitting the generation of pulse trains [62]. This dynamic control of magnetic mirror reflectivity potentially lends functionality to a range of spin-wave logic and memory devices.

A complete system of spin-wave logic based on dynamic current-controlled magnetic barriers has been proposed [63, 64]. Spin-wave logic is at an extremely early stage of development; indeed, apart from certain proof-of-concept studies, very little work has been done in this area. However, the technological potential of spin-wave information processing should not be overlooked, and—in terms of addressing the ongoing need for enhanced signal processing capability at lower energy cost—spin-wave technologies compare favourably with, for example, optical and magnetic contenders [65, 66].

Figure 3 shows a spin-wave NAND gate with a structure analogous to that of an optical Mach–Zehnder interferometer [64]. Two independent YIG waveguides each feature input and output antennas with a current-controlled mirror structure in between. Both channels are excited from a common pulsed supply with a relative phase of $2\pi/3$, and their outputs combined at a linear detector. The mirror currents I_1 and I_2 are the logical inputs, with zero current corresponding to a logical 0, and some current level I_S, a logical 1 [63, 64]. If both inputs are at logic 0, the output signal has a nonzero amplitude determined by the interference of the signals from the two channels at the detector. This is a logical 1 output state. By virtue of the relative phase of the two channels, this is the same output level which is observed if either I_1 or I_2 is at logic 1 (figure 3(*b*)). In the case that both inputs are logic 1, no spin waves reach the detector from either channel, and the output is logic 0. The NAND function belongs to the class of so-called universal logical functions, which means that any logical function can be realized by a combination of NAND gates. Spin-wave phase shifts, induced either by semi-transparent current-controlled mirrors [64] or intrinsic

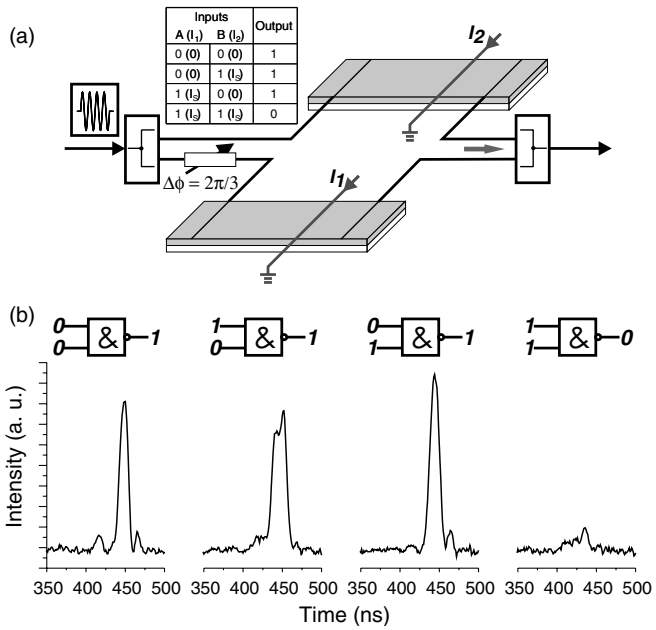

Figure 3. (*a*) Geometry of a spin-wave NAND gate. The currents I_1 and I_2 represent the logical inputs; the spin-wave interference signal represents the logical output. Inset: truth table for a NAND gate. (*b*) Gate output signals for input signals shown in the diagrams [64].

nonlinear material mechanisms, [67] have also been proposed as the basis of spin-wave logic platforms.

Several perspectives have been offered on approaches to integrated spin-wave logic. These include all-spin-wave information processing systems in which signals are carried and manipulated as spin-wave phases [68, 69]. As a practical step towards developing such concepts, an on-chip spin-wave combiner fabricated from a structured YIG waveguide, and capable of operating as a logical NOT gate has been reported [70].

3.3. Geometrically structured static magnonic crystals

Magnonic crystals (MCs)—artificial mesoscopic media with periodic lateral variations in their magnetic properties—are the microwave, magnetic analogue of photonic and sonic crystals. Spectra of spin-wave excitations in such structures are significantly different from those of uniform media and exhibit features such as band gaps, where spin wave propagation is entirely prohibited. Due to the wide tunability of their properties, these periodic structures are an excellent environment for the investigation of linear and nonlinear spin-wave dynamics.

Although the term magnonic crystal came into use only relatively recently, the first studies of spin-wave propagation in periodically structured YIG films were performed in the nineteen-seventies and nineteen-eighties. Various fabrication techniques were explored including geometric structuring, ion implantation, metallization and periodic magnetic biasing. Many interesting results were achieved (see for example the excellent review paper by Reed *et al* [71], Ishak [39] and also by Hartemann [72]), but the majority of the

studies performed at this time were functionally rather than phenomenologically motivated. Latterly, there has been a resurgence of interest in magnonic crystals and—for the first time—studies have been performed into the detailed physics of spin-wave propagation in these systems. Modern fabrication techniques enable the realization of a wide range of sophisticated engineered structures, and the device potential of micro- and nanoscaled MCs attracts increasing interest from the spintronic community [18–73]. Recent theoretical studies have made a very important contribution to this area [76–78].

Whilst from an applications perspective, attention is necessarily focused on very small-scale magnonic crystals, relatively large-sized (micrometre to millimetre) experimental YIG structures are—at least at the present time—the most valuable source of fundamental physical insight into the peculiarities of spin-wave behaviour in magnonic crystal systems.

Geometric structuring of a spin-wave waveguide is one of the simplest and most effective means to fabricate a magnonic crystal. Periodic patterning of a YIG film surface (i.e. variation of the waveguide thickness) is of particular interest (figure 4(*a*)) [79–81]. Early studies of structures of this type focused on MSSW and FVMSW scatter and propagation effects. Latterly, however, special attention has been turned towards BVMSW, owing to the unusual dispersion and nonlinear characteristics particular to this class of wave [82].

A geometrically patterned magnonic crystal is shown in figure 4(*a*). The fabrication method is a combination of photolithography and hot acid etching. A typical magnonic crystal might have an effective lattice constant of $\alpha = 300\,\mu$m, achieved via 20 parallel grooves of width $30\,\mu$m and separation $270\,\mu$m. It has been demonstrated that in the BVMSW configuration, a one-dimensional MC can achieve signal rejection over the magnonic band-gap region in excess of 30 dB [82]. The width of the rejection band and the rejection efficiency can be controlled by the groove depth [82, 83]. The optimal groove depth—for a combination of good rejection efficiency in the gap region and minimal insertion loss in the transmission bands—is found to be approximately one tenth of the total film thickness.

The dependence of MC rejection efficiency on the spin-wave geometry is particularly interesting. For a given crystal, it is found that the rejection efficiency for BVMSW is drastically higher than for MSSW [84]. Figure 4(*b*) shows data from a real experimental system, with a groove depth 500 nm (vertical dashed line) there is an approximately 28 dB (i.e. 600 fold) difference in rejection efficiency for the two wave types. The difference in behaviour is believed to be due to efficient two-magnon scattering of the directly excited, lowest order BVMSW mode to higher-order thickness modes. Subtleties such as these mean that developing a comprehensive understanding of magnonic crystal systems is an illuminating and highly nontrivial project.

The majority of work in the area of magnonic crystals has focused on investigating the properties of open-loop, externally driven systems. However, self-exciting positive-feedback

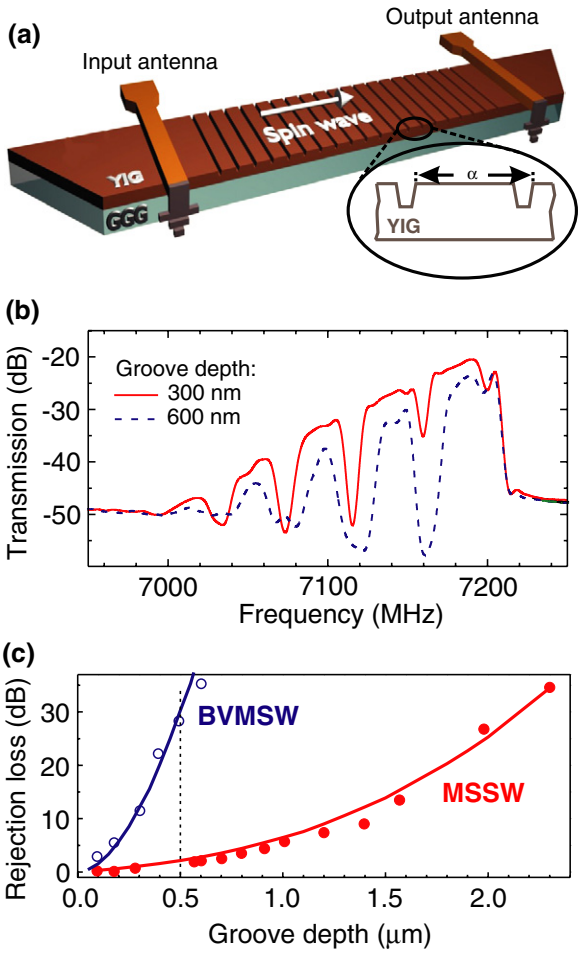

Figure 4. (*a*) Sketch of a magnonic crystal structure comprising an array of shallow grooves on a surface of a YIG film. (*b*) BVMSW microwave transmission characteristics for magnonic crystals for different groove depths. (*c*) Insertion loss in the rejection band measured for the BVMSW and MSSW geometries (open and filled symbols, respectively) as a function of the groove depth. The solid lines are the calculated insertion loss.

arrangements incorporating MCs provide useful additional physical insight. Recently, it was demonstrated that MCs can be used to achieve mode selection in spin-wave active rings [85].

Photolithography and wet etching have also been employed for the fabrication of two-dimensional (2D) YIG-based magnonic crystals [86, 87]. Work in this area is motivated by an interest in MCs which operate in conjunction with more than one direction of spin-wave propagation. Such systems are extremely challenging to realize, owing to the complex directional anisotropy of spin-wave spectrum: in a given crystal a demagnetizing field induced by the geometry of the crystal structure—in effect a form of mesoscopic artificial magnetocrystalline anisotropy—creates conditions of nonuniform internal field, and the spin-wave frequency depends strongly on the direction of propagation. Continued work in this area promises important future insight into the detailed physics of spin-wave propagation in structured magnetic films.

3.4. Dynamic and travelling magnonic crystals

As outlined in the previous section, research into the properties of geometric magnonic crystals has made an important contribution to the general field of spin-wave physics. A second class of magnonic crystal system—dynamic magnonic crystals—provides yet further insight and enables the observation of entirely new spin-wave phenomena.

The ability to vary the properties of a magnonic crystal on a timescale faster than the spin-wave relaxation time introduces the possibility of spin-wave storage and—in certain cases—access to physics which has significant and exciting implications not only for the field of spin-wave dynamics but also for wave physics in general. There are noteworthy parallels between this area and the emerging science of dynamic photonic crystals [88, 89].

Dynamic magnonic crystals (DMCs) are a relatively new area of research. The first fully functioning DMC was reported in 2009 [90]. The structure comprises a YIG waveguide placed in a spatially modulated, dynamically controllable magnetic field. This field is created by the superposition of an homogeneous bias and the localized Oersted field from a current-carrying meander structure positioned close to the YIG film surface, a thin spacer layer separates the two so as to prevent induction and re-radiation effects dominating the characteristics of the crystal (such effects limited the success of earlier structures [91, 92]). A well-defined rejection band is observed, the width and depth of which can be controlled via the current. A rejection band width of 30 MHz is readily attainable, and the crystal can be switched from full transmission to full rejection within 50 ns (approximately 10% of the spin-wave relaxation time).

Moving magnonic crystals are a sub-class of DMCs with transmission parameters which—rather than being simply switchable—vary continuously with time. Spin-wave reflections from a moving magnonic crystal are accompanied by a Doppler shift of the wave frequency. A moving magnonic crystal created in a YIG waveguide via the periodic strain induced by a travelling surface acoustic wave was reported in 2010 [93]. A special set of conditions on spin-wave wavenumber and frequency must be satisfied in order for spin-wave reflection from the structure to occur. Particularly noteworthy is the fact that the negative dispersion properties of BVMSW make it possible to observe a reverse Doppler shift in which waves (in this case, magnons) scattered from a receding reflector are shifted up in frequency and vice versa (i.e. the reverse of the acoustic Doppler phenomenon of everyday experience) [93].

4. Parametric amplification and wavefront reversal of spin waves

A parametric process is one in which a temporally periodic variation in some system parameter drives, brings about, or affects another coupled, temporally periodic process with a different characteristic time period. Parametric systems can be used to achieve amplification. Perhaps the most well known (and probably best appreciated) of all parametric amplifiers is the child's swing.

Parametric amplification processes feature widely in spin-wave systems and are among the most intricate of all magnon phenomena. In section 1 we offer a brief introduction to parametric processes in magnon systems. We go on to describe how parametric phenomena can be used for the amplification and wavefront reversal of spin-wave packets.

4.1. Parallel and perpendicular parametric pumping

The phenomenon of parametric instability in spin-wave systems was discovered by Bloembergen *et al* in 1952, through the observation of a nonlinear spin-wave damping effect [94, 95]. An explanation was later proposed by Anderson and Suhl [96] and a corresponding theory developed [97, 98]. The theory is based on a consideration of interactions between spin-wave eigenmodes in a system; specifically, between propagating modes and uniform precession (the $k = 0$ mode). When proper conditions are fulfilled, energy from a driven uniform precessional mode is able to feed into or 'pump' propagating modes, leading to their amplification from the thermal level. Since the alternating magnetization of the pumping mode in such a system is always perpendicular to the static bias field, this mechanism came to be known as spin-wave instability under perpendicular pumping.

The related but fundamentally physically distinct phenomenon of parallel pumping, discovered five years later by Shlömann *et al* [99], occurs when a spin-wave mode receives energy via a frequency-doubled alternating magnetic field applied along the magnetization direction. The main distinction between perpendicular and parallel pumping is that in the case of the latter, it is an alternating magnetic field which is responsible for the effect, rather than an alternating magnetization. In terms of energy quanta, parallel pumping can be understood as the creation of two magnons from a single pumping photon, whilst in the perpendicular case, amplification occurs by virtue of magnon-to-magnon splitting. The efficiency of parallel pumping can be superior to that of perpendicular pumping, owing to the fact that in the former, amplification is driven directly by magnons generated from the microwave photons from the pump, rather than indirectly from the splitting of magnons generated from the pumped $k = 0$ mode [100]. Parallel pumped systems are also attractive from an experimentalist's perspective, since the back-action of the pumped mode on the pump can generally be neglected. In this paper we focus attention mostly on parallel pumped systems.

The energy and momentum conservation laws for spin-wave instability under parallel pumping can be written as:

$$\begin{aligned} f_{m1} + f_{m2} &= f_p, \\ k_{m1} + k_{m2} &= k_p, \end{aligned} \tag{4}$$

where f_{m1}, f_{m2} and k_{m1}, k_{m2} are the energies and wavenumbers of the interacting magnons and f_p, k_p the frequency and wavenumber of the pump. From the energy conservation law, in the simplest case, the frequencies of the interacting magnons are both equal to half the pump frequency: $f_{m1} = f_{m2} = f_p/2$. The photon wavenumber is much smaller than that of the magnons ($k_p \ll k_{m1}, k_{m2}$), so that to a good approximation,

$k_{m1} = -k_{m2}$, implying that the interacting magnons are counter-propagating. In other words, the result of the process is the production of a secondary spin-wave packet (termed an idle packet) which is an amplified, phase conjugate version of the initial excitation. It has been demonstrated that this phenomenon can be used to perform wavefront reversal [101] which will be discussed in later sections.

Parametric instabilities are explored in detail in a number of excellent books, in particular we draw the interested reader's attention to [23] and chapter 10 in [44].

4.2. Amplification of spin-wave packets by parametric pumping

Practical use of spin waves as information carriers is strongly restricted (even in a low-damping material system such as YIG) by conversion losses and magnetic damping which cause relatively rapid attenuation of spin-wave signals in magnetic transmission lines. An ability to amplify spin-wave packets travelling in magnetic waveguides or magnonic crystals—and thus compensate for losses—is of crucial importance for further progress in magnonics.

Before we discuss the spin-wave amplification mechanism in most widespread use, parallel pumping using a pulsed microwave source, we review the various other available techniques.

A range of physical mechanisms for the amplification of travelling spin waves have been proposed and experimentally verified. These include quantum amplification of magnetostatic waves in ferrite-paramagnet structures [102, 103], amplification of magnetostatic waves via interaction with drifting carriers (see e.g. [104–109] as well as a review by Kazakov and Filimonov [110]), and parametric amplification. Further novel approaches to spin-wave amplification based, for example, on the spin-torque effect [111] or on the magnetoelectric interaction [112] have been considered theoretically, but have yet to be demonstrated experimentally.

In experiments on quantum amplification of FVMSW in a composite structure of YIG and $Al_2O_3 : Cr^{3+}$ (ruby) a maximum amplification coefficient of 25 dB was demonstrated at signal frequency 6.1 GHz. However, owing to the practical challenges of this technique (liquid helium temperatures and very high-frequency (cited 35.52 GHz) pumping of the ruby crystal) it has not been widely adopted. The amplification coefficient decreases from 25 to 12 dB with an increase in temperature from 1.6 to 4.2 K [103]. Moreover, no MSW amplification was observed in an epitaxial structure comprising a conventional YIG film grown on a gadolinium gallium garnet $Gd_3Ga_5O_{12}$ (GGG) substrate, which is explained by a strong paramagnetic absorption of MSWs in the GGG crystal at low temperatures.

In spite of that fact that theoretical estimations predict a high dB mm^{-1} amplification figure (see, e.g. [107]) through interactions between MSWs and drifting carriers, no work has been done in this area recently. The best result was reported in [109] where a relative gain of 17 dB was observed for MSSWs propagating at 4.2 GHz in a thick YIG slab. The slab was positioned near the surface of a GaAs layer where the charge flow was driven by an extremely high external voltage (700 V). However, this gain was hardly enough to compensate for the additional loss caused by interaction between the MSW system and the electronic structure of the semiconductor. In [107, 108] it is theoretically predicted that in thick samples the amplification frequency bandwidth of this technique is very small and the amplification figure critically dependent on charge velocity, semiconductor conductivity and magnetic losses. Though the situation in thin magnetic films looks to be more favourable, no such experiments are known to the authors. Heating of the current-carrying structure, proper coupling of MSWs with drifting carriers and additional damping in semiconductors are among many additional technical problems and limitations.

Accordingly, at the present time, parametric amplification is the only widespread technique for the amplification of both linear and nonlinear spin-wave packets in YIG films.

Parametric amplification experiments involve spin waves with frequencies ranging from a few gigahertz to a few tens of gigahertz. Maximum gains achieved at room temperature exceed 30 dB. The first success in parametric amplification of magnetoelastic and magnetostatic modes was achieved in an axially magnetized single crystal YIG rod at frequency 8.7 GHz at 1.5 K [113] using perpendicular parametric pumping. A travelling spin-wave packet was exited at one end of the structure and allowed to propagate to the other where it was then pumped by a pulse of double the signal frequency, 1 μs duration, and 500 W peak power. The power of the reflected and amplified spin-wave pulse subsequently detected at the input was as much as 35 dB higher than that of the source excitation. The counter-propagating idle spin-wave packet created by pump during the amplification process was also detected [114].

The amplification of travelling MSSW [115, 116] and BVMSW [117–119] magnetostatic waves in the YIG film waveguides by a localized parallel microwave magnetic pumping field has been demonstrated. It is also possible to realize amplification of a weak FVMSW excitation by a strong one through a nonlinear four-wave parametric process [120]. In this case, both waves propagate in the YIG film at adjacent frequencies lying in a highly dispersive region of the dipole-exchange spin-wave spectrum.

It is necessary to note that all experiments on spin-wave amplification by an external pumping field are performed in a regime of pulsed (as opposed to continuous) pumping. Owing to the multi-mode character of the magnon spectrum, this is of paramount importance for the amplification process. Due to frequency degeneracy of a long wavelength signal wave and other short wavelength exchange-dominated spin-wave eigenmodes in ferromagnetic materials, if frequency-selective amplification is to be achieved, the pumping must not be stationary. When strong pumping is applied, parametrically excited exchange spin-wave modes are unstable, and their amplitudes start to grow exponentially from the thermal level. A finite time is necessary for them to grow to magnitudes at which they can significantly affect the propagation of a MSW signal packet [115, 117]. This growth time depends on the pumping amplitude and can range from several hundred

nanoseconds to several microseconds. In order to prevent the growth of these exchange spin waves to experimentally detectable levels, and thus avoid undesirable competition with an amplified signal packet, the pumping duration must be made considerably shorter than their characteristic relaxation time [121].

A further important parameter influencing the amplification process is the spatial extent of the pumping field. Spin-wave energy flow out of a spatially restricted pumping area is equivalent to an additional loss term affecting the amplified spin wave. As a result, the threshold of parametric generation for the wave increases and the amplification figure decreases [100, 116, 122]. Moreover, the interaction time between the travelling spin-wave packet and the pump is limited to that taken for the pulse to propagate through the pump area. In the work of Melkov *et al* [121] a detailed theoretical and experimental study of parametric interaction of magnetostatic waves with a localized, nonstationary pump is presented. The effect of the parametric excitation of exchange spin waves on the interaction of backward volume magnetostatic waves with a localized nonstationary parametric pump is determined both for large, $l \gg \lambda$ and small $l < \lambda$ pump regions (λ being the BVMSW wavelength). In the case of large pumping regions, the interaction of a signal wave with a nonstationary pump has some nontrivial consequences, namely compression of the signal pulse, and a distortion of the amplitude profile which shifts the position of the peak. It is also established that using nonstationary pumping makes it possible to increase the pump power significantly above the threshold for generation (i.e. pumping from the thermal level as opposed to amplification of the signal) in the stationary regime, enabling much higher gains [121].

Even more interesting results are observed in the case of so-called nonadiabatic parametric interactions [123]. Here, parametric pumping is localized to a region with a length which is at least as small as the MSW wavelength. The unusual feature of nonadiabatic three-wave parametric interactions is the simultaneous excitation of two idle wavepackets, one co- the other counter- propagating relative to the original excitation (see next section for further detail). If the phase difference between the signal and pumping at the moment of their interaction in the localized pumping region is not well defined [123], the interference between these two signals leads to strong beating of the amplified signal. External locking of signal and pumping phases permits control of the amplitude of the amplified output signal from a maximum to zero gain level [124]. This effect can be exploited for phase selection of nonlinear spin-wave eigenmodes in self-exciting positive-feedback spin-wave systems [125–127].

The amplification of nonlinear eigenexcitations of magnetic media, namely spin-wave envelope solitons [128, 129] and bullets [53–130], constitutes a very interesting and important separate problem [117, 118]. It is well known that amplification of a spin-wave soliton by an ideal linear amplifier is not possible above 6 dB [132]. Above this level of gain, fundamental single solitons split into two parts, distorting the spin-wave information they carry in the process. The solution is to provide simultaneously both amplification and compression [132, 133]. This can be realized by localized pulsed parametric pumping. Using this technique, an amplification of 17 dB of fundamental BVMSW solitons has been demonstrated [133].

4.3. Spin-wave wavefront reversal by parallel pumping

In this section, the nonlinear phenomena of wavefront reversal (WFR) (also known as phase conjugation) and time inversion of dipolar spin-wave pulses are reviewed [101, 134–136]. Spin-wave WFR happens as a result of a nonstationary three-wave parametric interaction with parallel electromagnetic pumping.

Wavefront reversal (or phase conjugation) phenomena differ from simple wave reflection processes in many important respects (see, e.g. [137]). Whilst the direction of a reflected wave is determined by Snell's law, a reversed wave always propagates in the direction opposite to that of the source excitation. Moreover, under certain reversal conditions, the leading front of the source (incident) waveform is transformed into the trailing front of the reversed excitation, i.e. the time profile of the reversed waveform is an inverted version of the original. The effect of pulse profile time reversal has been well demonstrated in experiments involving two parametrically pumped pulses of different amplitudes [121, 134] (figure 5(*a*)) and the phenomenon has also been observed in two-dimensional systems by BLS spectroscopy (figure 5(*b*)) [138].

Nonlinear optical wavefront reversal has long been a subject of interest [137]. The process of optical parametric WFR, however, is distinct from that observed in magnon systems. Optical processes involve second-order, four-wave parametric interactions, pumped by counter-propagating light waves with frequencies close to those of the source and reversed signals. Spin-wave systems provided the first experimental evidence of WFR through a first-order three-wave parametric process.

Wavefront reversal of nonreciprocal surface spin waves (MSSW) has additional, interesting features. Here, the process of parametric interaction is complicated by the fact that counter-propagating MSSWs are localized to different film surfaces, reducing the effective interacting cross section. It has been shown that WFR of MSSW can be achieved, but its efficiency decreases with increasing surface mode localization which is determined in turn by the wavenumber [139, 140].

Wavefront reversal of dipolar-exchange spin waves (DESWs) is of special interest, and will be discussed in the next section. It has been shown that in the case of DESW, the use of additional pump pulses allows double and multiple wavefront reversal processes to be observed.

5. Storage and recovery phenomena in multi-mode spin-wave systems

As elucidated in previous sections, the spectrum of spin-wave eigenexcitations in a real ferromagnetic system is very rich. It consists of an intricate tapestry of coupled uniform, standing and propagating modes of different wavevectors and frequencies. Energy and information externally inserted

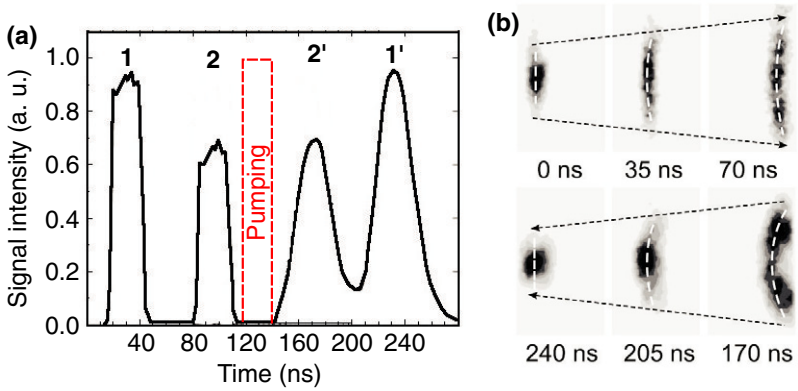

Figure 5. (*a*) Reversal of the time profile of a spin-wave signal. 1, 2: signals reflected from the input transducer before interaction with pumping. 1′, 2′: signals at the input transducer created by the reversed wave formed in a parametric interaction with pumping. (*b*) Wavefront reversal of a two-dimensional spin-wave packet. The two-dimensional spatial distributions of the spin-wave pulse intensity are captured at successive moments in time using the time-resolved BLS technique. The pump signal was applied during the time interval from 78 to 156 ns. The wave front of the incident pulse that is slightly concave before the interaction with pumping becomes clearly convex after the interaction and change in the propagation direction [138].

into a spin-wave system may be distributed over and transferred between many modes. Mechanisms of linear and nonlinear modal coupling provide the possibility of storage and recovery of spin-wave information. An exploration of these mechanisms is the subject of the following section.

5.1. Spin-wave echo and wavefront reversal of DESWs

In general terms, an echo involves the spontaneous reappearance of a coherent response (or output) of some excited system after the coherence of the source—an initial coherent excitation—has been lost or decayed. It is important to note that an echo is first and foremost a phase-related phenomenon. The key mechanism in echo formation is dephasing; damping (i.e. energy decay)—if present at all—plays only a minor role [141].

The response of a general multi-mode system to a pulsed excitation decays via a mechanism known as phase relaxation. The system can be modelled as a network of weakly coupled oscillators. The ensemble of oscillators has some statistical distribution of characteristic frequencies, so that if initially forced to oscillate coherently by an external excitation, when that excitation is removed, the system gradually dephases and—after some characteristic time period—the macroscopic (net) signal is zero. This process is shown schematically in figure 6(*a*). The left-hand diagram represents an initial, entirely phase coherent state of the system corresponding to a time $t = 0$. With time, the phases of oscillators in the ensemble with characteristic frequencies higher than the mean value ($\Delta f_k = 0$) increase (solid arrows), and the phases of those with lower frequencies decrease (dashed arrows). Thus, there comes some time $t = T_p$ at which phase coherence is entirely lost, and the macroscopic signal is accordingly zero.

In most physical systems when modes are excited over a wide frequency band, phase relaxation occurs on a timescale which is much faster than energy damping so that excitations of finite amplitude still exist after coherence has been lost (in other words, at least for some time after it has evolved, the zero net excitation in the dephased state is a non-trivial sum). Under certain conditions, in such a system, the application of a second excitation—a pump pulse—(see figure 6(*b*)) can precipitate the conversion of the existing oscillations into a new set with the same frequencies but with conjugate initial phases (see dashed and solid arrows in the figure). The subsequent evolution of these signals (the reverse of the original dephasing evolution) then results in the restoration of the original signal. If pump pulse is applied at time T_p, restoration is observed at $2T_p$.

Echo phenomena have been studied in detail in many physical systems [141]. Observation of a spin-wave echo (or magnetostatic mode echo) brought about via two external pumping pulses of the same frequency was first reported in 1965 [142] and over the last forty years a high level of understanding of the detailed physics of the mechanism has been attained (see for example [143–146] and references therein). Many theoretical models have been developed to explain the spin-wave echo phenomenon [144–146]. In order for phase relaxation to take place, these require the presence of many spatially localized spin-wave modes with different frequencies. In order to realize such a situation experimentally, a nonuniform internal magnetic field and pulsed input signal are generally required. It has also been discovered that slow BVMSW at the bottom of the magnon spectrum, which can be effectively excited in conditions of nonuniform magnetic bias field near the edges of bulk samples, and slow MSSW existing in uniformly magnetized YIG films just above the frequency of ferromagnetic resonance [147] can participate in the echo process.

Signal restoration can be achieved by perpendicular pumping where—by analogy with the wavefront reversal process described in section 4.3—the perpendicular pump generates a set of phase conjugate oscillations [143–147]. Two features distinguish such an echo from, for example, nuclear or paramagnetic spin echoes. Firstly, the echo amplitude has a nonmonotonic dependence on time T_p. Secondly, the echo amplitude can exceed the amplitude of the first pulse (for example in bulk YIG samples the echo gain can be as large as 50 dB [143]). Both these features are caused by energy

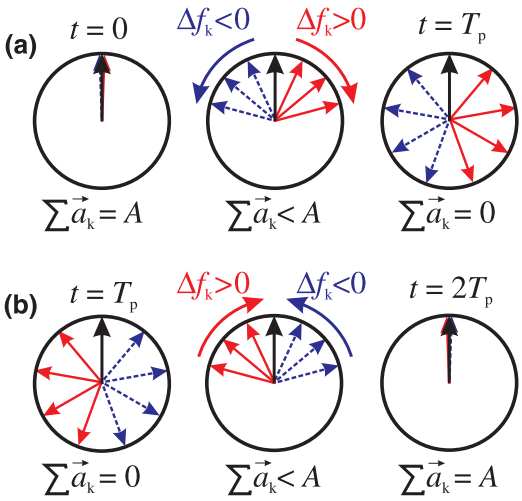

Figure 6. (*a*) Phase relaxation in a system of coupled oscillators with characteristic frequencies distributed about a mean value. After some time T_p the system loses coherence and the macroscopic oscillation signal is equal to zero (right). (*b*) Phase evolution in an echo event. A phase conjugate signal is generated by a pump pulse at time T_p (compare dashed and solid arrows with figure (*a*)), resulting in the restoration of the signal at time $2T_p$. Here, a_k are the amplitudes of individual oscillator responses and A is their summation (the net, macroscopic signal).

transfer from the pump pulse in a second order parametric process [144, 148].

First-order parametric processes constitute a separate class of spin-wave echoes. In YIG spheres, two-magnon scattering of an initially excited uniform precessional mode excites a set of dipolar-exchange spin waves (DESW) with almost zero group velocities. The signal arising from these waves vanishes rapidly through phase relaxation but can be recovered via wavefront reversal driven by parallel pumping. Re-established DESWs are then, in turn, scattered back into the uniform precessional mode, resulting in its partial restoration [149]. It has been shown that an increase in the restoration efficiency can be achieved by scratching the YIG surface to increase the density of scattering centres [149].

Generally, two-magnon elastic scattering processes are undesirable in magnonic devices because they result in additional spin-wave damping [150]. However—as in the example of the sphere given above—in pumped systems, such mechanisms can play a useful energy-transfer role [151]. This theme has been explored in the literature, particularly in the context of dipolar-exchange spin-wave based signal processing in YIG films [151–153]. The concept is to convert energy in the form of readily excited MSW modes to low velocity and low-damping DESW modes which are highly attractive for information transfer and storage purposes. In such systems, for ease of signal reception, wavefront reversal by parallel pumping has been proposed as a means to reconvert DESW back into MSW. After wavefront reversal, each DESW generated in the two-magnon scattering process propagates back along the same trajectory, so that all these waves are scattered back into MSW.

In a conventional spin-wave transmission structure, the delay between signal excitation and reception is determined

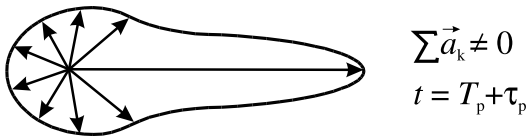

Figure 7. Restoration of a macroscopic signal from a dephased stat by means of a frequency-selective amplification. The diagram illustrates the asymmetric state of the system after frequency-selective amplification. T_p is the time of amplification switching, τ_p the amplification duration.

by the distance between the input and output antennas and the group velocity, and in typical experimental structures is of the order of hundreds of nanoseconds. Wavefront reversal of low-velocity DESW modes allows this delay time to be increased to up to 2.6 μs [153]. Moreover, it has been demonstrated that double and multiple DESW wavefront reversal processes driven by multiple pulse pumps can be used to extend spin-wave information storage times infinitely [154, 155].

5.2. Reversal of spin-wave momentum relaxation

In the last section we discussed phase conjugation based reversal of phase relaxation and signal restoration in spin-wave systems. In 2001, a fundamentally different method of signal restoration was proposed [156]. It was demonstrated that the coherence of a dephased state can be restored by frequency-selective amplification of waves (or oscillations) with frequencies close to that of the original excitation. This process was known as reversal of momentum relaxation.

Momentum relaxation reversal is illustrated schematically in figure 7. As discussed in the previous section (see figure 6(*a*)), after some characteristic time period, the macroscopic response from an initially phase coherent system of nonidentical weakly coupled oscillators decays to zero through phase relaxation. Application of a frequency-selective amplifier to the decoherent system results in a strong preferential increase in the amplitudes of spin waves of a certain frequency (or over a narrow frequency range) and phase. As a result, the symmetry of the phase distribution in the system is broken, and the net signal is nonzero. The restored signal is a maximum at the point when the amplification is switched off. This phenomenon earns its place in this section since here—like in the spin-wave echo systems described in the previous section—transfer of energy between spin-wave modes plays a pivotal role.

It has been demonstrated that parallel parametric pumping can be used as the basis for momentum relaxation reversal [156]. In fact, this mechanism is ideally suited to the purpose: its amplification efficiency is maximal for spin waves at half the pumping frequency, and decreases with detuning from this value [121].

A combination of reversal of momentum relaxation and spin-wave wavefront reversal has also been reported [157]. Here, a single pumping excitation drives both effects. Under certain conditions it is possible to observe a restored signal which has the form of two time-separated pulses: one originating from momentum relaxation reversal, the other from the phase conjugation process. A short pump pulse is

preferable for the restoration of a signal using the mechanism of phase conjugation, whilst long ones (with narrow spectra) are more suitable for momentum relaxation reversal [157].

5.3. Parametric restoration of spin-wave signals stored in standing dipolar-exchange modes

As discussed in the earlier part of this section, the storage of microwave information in standing (or very slow) spin-wave modes attracts significant interest. This section is devoted to the storage and parametric recovery of spin-wave signals stored in dipolar-exchange standing thickness modes [47] of a thin YIG film.

In any thin-film spin-wave system, discrete, short wavelength, exchange-dominated standing thickness modes exist. The dispersion curves associated with these modes intersect those of MSSW. Band gaps open up at the dispersion crossing points, and these band gaps—which are associated with zero wave velocities—can be used for the storage of the information [47].

When a MSSW packet with a carrier frequency close to a known dipole-exchange mode is excited in and travels through a waveguide, it interacts with standing modes as it propagates, leaving a 'trail' of perpendicular excitations in its wake. After the initial excitation has passed, a long, powerful pumping pulse can be used to increase the amplitudes of the residual standing mode excitations, and transfer energy back into a restored propagating surface mode [158–160]. Parallel parametric pumping is again used for the recovery of the stored spin-wave signal, but here the mechanism is different from that described in the previous two sections. Phase relaxation is not relevant (since the stored signal is by nature monochromatic) and simple parametric amplification plays the dominant role.

A distinguishing feature of this type of storage-recovery mechanism is that the restoration of the signal takes place whilst the pump is still active. As a consequence, amplification is effective only over a certain finite time period, after which saturation occurs and standing modes are suppressed. The process is well modelled by a system of two competing spin-wave groups, both of which interact with the pump signal. In the saturated regime, only one spin-wave group can exist [23]. This group—the dominant group—suppresses all other spin-wave modes. As a result, the amplification of the standing mode prior to saturation and its suppression afterwards results in the appearance of broad restored signal [158]. A detailed theoretical model explaining this mechanism has been developed [159]. In addition, nonresonant parametric recovery—in which the input signal frequency is detuned from half of the pumping frequency—has been used to perform spectral analysis of the stored microwave signal [160].

The storage-recovery mechanisms explored in this section serve to highlight the diversity, subtlety and inter-connectivity of the dynamic effects observed in multi-mode magnon systems. It is only through the extraordinary properties of yttrium iron garnet: its wide spectrum of spin-wave eigenexcitations and pronounced nonlinear properties that we have the opportunity to model and study such challenging and fascinating physical phenomena.

6. Conclusions

In this paper we have reviewed several important directions in the study of linear and nonlinear spin-wave dynamics in yttrium iron garnet. We have endeavoured to focus on the main challenges in modern magnonics, exploring key aspects of the transport, storage and processing of microwave and digital information in multi-modal spin-wave systems. Nevertheless, the results highlighted here are not limited to issues of practical application. Our main aim was to try to combine a coherent account of progress in magnonics over the last two decades with a perspective on how the various aspects of diverse physical phenomena accessible in these fascinating magnetic systems relate to modern information processing methodologies.

Acknowledgments

The authors thank Alexy Karenowska for strong support in the preparation of this paper.

References

[1] Hillebrands B 1990 *Phys. Rev.* B **41** 530
[2] Hillebrands B, Harzer J V, Güntherodt G, England C D and Falco C M 1990 *Phys. Rev.* B **42** 6839
[3] Kolodin P A and Hillebrands B J 1996 *J. Magn. Magn. Mater.* **161** 199
[4] Hillebrands B, Mathieu C, Bauer M, Demokritov S O, Bartenlian B, Chappert C, Decanini D, Rousseaux F and Carcenac F 1997 *J. Appl. Phys.* **81** 4993
[5] Kruglyak V V and Hicken R J 2006 *J. Magn. Magn. Mater.* **306** 191
[6] Neusser S, Botters B and Grundler D 2008 *Phys. Rev.* B **78** 054406
[7] De Gennes P G, Pincus P A, Hartman-Boutron F and Winter M 1963 *Phys. Rev.* **129** 1105
[8] Andrienko A V, Ozhogin V I, Safonov V L and Yakubovskiĭ A Yu 1991 *Sov. Phys.—Usp.* **34** 843
[9] Svistov L E, Löw J and Benner H 1993 *J. Phys.: Condens. Matter* **5** 4215
[10] Andrienko A V 2005 *J. Exp. Theor. Phys.* **100** 77
[11] Schultheiss H, Schäfer S, Candeloro P, Leven B, Hillebrands B and Slavin A N 2008 *Phys. Rev. Lett.* **100** 047204
[12] Demidov V E, Demokritov S O, Rott K, Krzysteczko P and Reiss G 2008 *Appl. Phys. Lett.* **92** 232503
[13] Demidov V E, Jersch J, Demokritov S O, Rott K, Krzysteczko P and Reiss G 2009 *Phys. Rev.* B **79** 054417
[14] Demidov V E, Jersch J, Rott K, Krzysteczko P, Reiss G and Demokritov S O 2009 *Phys. Rev. Lett.* **102** 177207
[15] Patton C E 1968 *J. Appl. Phys.* **39** 3060
[16] Heinrich B and Frait Z 1966 *Phys. Status Solidi* B **16** K11
[17] Demidov V E, Demokritov S O, Rott K, Krzysteczko P and Reiss G 2008 *J. Phys. D: Appl. Phys.* **41** 164012
[18] Chumak A V *et al* 2009 *Appl. Phys. Lett.* **95** 262508
[19] Geller S and Gilleo M A 1957 *Acta Crystallogr.* **10** 239
[20] Cherepanov V, Kolokolov I and L'vov V 1993 *Phys. Rep.—Rev. Sec. Phys. Lett.* **229** 81
[21] Winkler G 1981 *Magnetic Garnets* (Braunschweig, Wiesbaden: Vieweg)
[22] Wigen P E 1994 *Nonlinear Phenomena and Chaos in Magnetic Materials* (Singapore: World Scientific)
[23] L'vov V S 1994 *Wave Turbulence under Parametric Excitations: Applications to Magnetics* (Berlin: Springer)

[24] Cottam M G 1994 *Linear and Nonlinear Spin Waves in Magnetic Films and Superlattices* (Singapore: World Scientific)
[25] Shrinivasan G and Slavin A N 1995 *High Frequency Processes in Magnetic Materials* (Singapore: World Scientific)
[26] Stancil D D and Prabhakar A 2009 *Spin Waves Theory and Applications* (New York: Springer)
[27] Rodrigue G P 1988 *Proc. IEEE* **76** 121
[28] Schlömann E F 1988 *Proc. IEEE* **76** 188
[29] Krishnan R, LeGall H and Vien T K 1973 *Phys. Status Solidi* A **17** K65
[30] Wettling W 1975 *Appl. Phys. A—Mater. Sci. Process.* **6** 367
[31] Cooper R W, Crossley W A, Page J L and Pearson R F 1968 *J. Appl. Phys.* **39** 565
[32] Demokritov S O, Hillebrands B and Slavin A N 2001 *Phys. Rep.—Rev. Sec. Phys. Lett.* **348** 441
[33] Nielsen J W and Dearborn E F 1958 *J. Phys. Chem. Solids* **5** 202
[34] Laudise R A 1970 *The Growth of Single Crystals* (Englewood Cliffs, NJ: Prentice-Hall)
[35] Levinstein H J, Licht S, Landorf R W and Blank S L 1971 *Appl. Phys. Lett.* **19** 486
[36] Blankand S L and Nielsen J W 1972 *Cryst. Growth* **17** 302
[37] Glass H L 1988 *Proc. IEEE* **76** 151
[38] Adam J D 1988 *Proc. IEEE* **76** 159
[39] Ishak W S 1988 *Proc. IEEE* **76** 171
[40] Eshbach J R and Damon R W 1960 *Phys. Rev.* **118** 1208
[41] Damon R W and Eshbach J R 1961 *J. Phys. Chem. Solids* **19** 308
[42] Damon R W and Van De Vaart H 1965 *J. Appl. Phys.* **36** 3453
[43] Stancil D D 1993 *Theory of Magnetostatic Waves* (New York: Springer)
[44] Gurevich A G and Melkov G A 1996 *Magnetization Oscillations and Waves* (New York: CRC Press)
[45] Zavislyak I V and Tychynskiy A V 1989 *Physical Concepts in Functional Microelectronics* (Kiev: UMK VO) (in Russian)
[46] Kalinikos B A 1980 *IEE Proc. H—Microw. Opt. Antennas* **127** 4
[47] Kalinikos B A and Slavin A N 1986 *J. Phys. C: Solid State Phys.* **19** 7013
[48] Schneider T, Kostylev M P, Serga A A, Neumann T and Hillebrands B 2008 *Phys. Rev.* B **77** 214411
[49] Demidov V E, Kostylev M P, Rott K, Krzysteczko P, Reiss G and Demokritov S O 2009 *Appl. Phys. Lett.* **95** 112509
[50] Demidov V E, Demokritov S O, Hillebrands B, Laufenberg M and Freitas P P 2004 *Appl. Phys. Lett.* **85** 2866
[51] Serga A A, Schneider T, Hillebrands B, Demokritov S O and Kostylev M P 2006 *Appl. Phys. Lett.* **89** 063506
[52] Fohr F, Serga A A, Schneider T, Hamrle J and Hillebrands B 2009 *Rev. Sci. Instrum.* **80** 043903
[53] Serga A A, Kostylev M P and Hillebrands B 2008 *Phys. Rev. Lett.* **101** 137204
[54] Eshbach J R 1962 *Phys. Rev. Lett.* **8** 357
[55] Schlömann E and Joseph R I 1964 *J. Appl. Phys.* **35** 167
[56] Demokritov S O, Serga A A, André A, Demidov V E, Kostylev M P, Hillebrands B and Slavin A N 2004 *Phys. Rev. Lett.* **93** 047201
[57] Kostylev M P, Serga A A, Schneider T, Neumann T, Leven B, Hillebrands B and Stamps R L 2007 *Phys. Rev.* B **76** 184419
[58] Neumann T, Serga A A, Hillebrands B and Kostylev M P 2009 *Appl. Phys. Lett.* **94** 042503
[59] Demidov V E, Hansen U H and Demokritov S O 2008 *Phys. Rev.* B **78** 054410
[60] Hansen U-H, Gatzen M, Demidov V E and Demokritov S O 2007 *Phys. Rev. Lett.* **99** 127204
[61] Schneider T, Serga A A, Chumak A V, Hillebrands B, Stamps R L and Kostylev M P 2010 *Europhys. Lett.* **90** 27003
[62] Serga A A, Neumann T, Chumak A V and Hillebrands B 2009 *Appl. Phys. Lett.* **94** 112501
[63] Kostylev M P, Serga A A, Schneider T, Leven B and Hillebrands B 2005 *Appl. Phys. Lett.* **87** 153501
[64] Schneider T, Serga A A, Leven B, Hillebrands B, Stamps R L and Kostylev M P 2008 *Appl. Phys. Lett.* **92** 022505
[65] Karim Mohammed A and Abdul Awwall A S 1992 *Optical Computing: An Introduction* (New York: Wiley)
[66] Allwood D A, Xiong G, Faulkner C C, Atkinson D, Petit D and Cowburn R P 2005 *Science* **309** 1688
[67] Hansen U-H, Demidov V E and Demokritov S O 2009 *Appl. Phys. Lett.* **94** 252502
[68] Khitun A and Wang K L 2005 *Superlatt. Microstruct.* **38** 184
[69] Khitun A, Bao M and Wang K L 2008 *IEEE Trans. Magn.* **44** 2141
[70] Kostylev M, Schneider T, Serga A and Hillebrands B 2008 *J. Nanoelectron. Optoelectron.* **3** 69
[71] Reed K W, Owens J M and Carter R L 1985 *Circ. Syst. Sign. Proc.* **4** 157
[72] Hartemann P 1984 *IEEE Trans. Magn.* **MAG-20** 1272
[73] Gubbiotti G, Tacchi S, Carlotti G, Singh N, Goolaup S, Adeyeye A O and Kostylev M 2007 *Appl. Phys. Lett.* **90** 092503
[74] Kostylev M, Schrader P, Stamps R L, Gubbiotti G, Carlotti G, Adeyeye A O, Goolaup S and Singh N 2008 *Appl. Phys. Lett.* **92** 132504
[75] Wang Z K, Zhang V L, Lim H S, Ng S C, Kuok M H, Jain S and Adeyeye A O 2009 *Appl. Phys. Lett.* **94** 083112
[76] Lee K S, Han D S and Kim S K 2009 *Phys. Rev. Lett.* **102** 127202
[77] Krawczyk M and Puszkarski H 2008 *Phys. Rev.* B **77** 054437
[78] Kruglyak V V, Hicken R J, Kuchko A N and Gorobets V Y 2005 *J. Appl. Phys.* **98** 014304
[79] Skyes C G, Adam J D and Collins J H 1976 *Appl. Phys. Lett.* **29** 388
[80] Parekh J P and Tuan H S 1977 *Appl. Phys. Lett.* **30** 667
[81] Parekh J P and Tuan H S 1978 *IEEE Trans. Microw. Theory Tech.* **26** 1039
[82] Chumak A V, Serga A A, Hillebrands B and Kostylev M P 2008 *Appl. Phys. Lett.* **93** 022508
[83] Chumak A V, Serga A A, Wolff S, Hillebrands B and Kostylev M P 2009 *J. Appl. Phys.* **105** 083906
[84] Chumak A V, Serga A A, Wolff S, Hillebrands B and Kostylev M P 2009 *Appl. Phys. Lett.* **94** 172511
[85] Karenowska A D, Chumak A V, Serga A A, Gregg J F and Hillebrands B 2010 *Appl. Phys. Lett.* **96** 082505
[86] Gulyayev Yu V, Nikitov S A, Zhivotovskii L V, Klimov A A, Tailhades Ph, Presmanes L, Bonningue C, Tsai C S, Vysotskii S L and Fillimonov Yu A 2003 *JETP Lett.* **77** 567
[87] Vysotskii S L, Nikitov S A and Filimonov Yu A 2005 *JETP* **101** 636
[88] Tanaka Y, Upham J, Nagashima T, Sugiya T, Asano T and Noda S 2007 *Nature Mater.* **6** 862
[89] Bravo-Abad J and Soljacic M 2007 *Nature Mater.* **6** 799
[90] Chumak A V, Neumann T, Serga A A, Hillebrands B and Kostylev M P 2009 *J. Phys. D: Appl. Phys.* **42** 205005
[91] Myasoedov A N and Fetisov Y K 1989 *Sov. Phys.—Tech. Phys.* **34** 666
[92] Fetisov Y K, Ostrovskaya N V and Popkov A F 1996 *J. Appl. Phys.* **79** 5730
[93] Chumak A V, Dhagat P, Jander A, Serga A A and Hillebrands B 2010 *Phys. Rev.* B **81** 140404
[94] Blombergen N and Damon R W 1952 *Phys. Rev.* **85** 699
[95] Blombergen N and Wang S 1954 *Phys. Rev.* **93** 72
[96] Anderson P W and Suhl H 1955 *Phys. Rev.* **100** 1788
[97] Suhl H 1956 *Proc. IRE* **44** 1270
[98] Suhl H 1957 *J. Phys. Chem. Solids* **1** 209
[99] Schlömann E, Green J J and Milano U 1960 *J. Appl. Phys.* **31** 386S

[100] Neumann T, Serga A A, Vasyuchka V I and Hillebrands B 2009 *Appl. Phys. Lett.* **94** 192502
[101] Gordon A L, Melkov G A, Serga A A, Slavin A N, Tiberkevich V S and Bagada A V 1998 *JETP Lett.* **67** 913
[102] Balinskii M G, Danilov V V and Nechiporuk A Y 1993 *Zh. Techn. Fiz.* **63** 122
[103] Danilov V V and Nechiporuk A Y 2002 *Techn. Phys. Lett.* **28** 369
[104] Schlömann E 1969 *J. Appl. Phys.* **40** 1422
[105] Vashkovskii A V, Zubkov V I, Kildishev N and Murmuzhev B A 1972 *JETP Lett.* **16** 2
[106] Kawasaki K, Takagi H and Umeno M 1974 *IEEE Trans. Microw. Theory Tech.* **MTT-22** 918
[107] Bini M, Millanta L and Rubino N 1978 *IEEE Trans. Magn.* **MAG-14** 811
[108] Bini M, Filetti P L, Millanta L and Rubino N 1978 *J. Appl. Phys.* **49** 3554
[109] Yamada S, Chang N S and Matsuo Y 1982 *J. Appl. Phys.* **53** 5979
[110] Kazakov G T and Filimonov Yu A 1989 *Russ. Phys. J.* **32** 1
[111] Seo S-M, Lee K-J, Yang H and Ono T 2009 *Phys. Rev. Lett.* **102** 147202
[112] Khitun A, Nikonov D E and Wang K L 2009 *J. Appl. Phys.* **106** 123909
[113] Damon R W and Van De Vaart H 1965 *Appl. Phys. Lett.* **6** 152
[114] Van De Vaart H 1966 *IEEE Trans. Son. Ultrason.* **su-13** 84
[115] Vashkovskii A V, Zubkov V I, Krutzenko I V and Melkov G A 1984 *JETP Lett.* **39** 146
[116] Melkov A and Sholom S V 1990 *Sov. Phys.—Tech. Phys.* **35** 943
[117] Bagada A V, Melkov G A, Serga A A and Slavin A N 1997 *Phys. Rev. Lett.* **79** 2137
[118] Kolodin P A, Kabos P, Patton C E, Kalinikos B A, Kovshikov N G and Kostylev M P 1998 *Phys. Rev. Lett.* **80** 1976
[119] Melkov G A, Serga A A, Tiberkevich V S, Oliynyk A N, Bagada A V and Slavin A N 1999 *IEEE Trans. Magn.* **35** 3157
[120] Kalinikos B A, Kovshikov N G, Kostylev M P and Benner H 1996 *JETP Lett.* **64** 171
[121] Melkov G A, Serga A A, Slavin A N, Tiberkevich V S, Oleinik A N and Bagada A V 1999 *JETP* **89** 1189
[122] Gorbunov L M 1974 *Sov. Phys.—JETP* **40** 689
[123] Melkov G A, Serga A A, Tiberkevich V S, Kobljanskij Yu V and Slavin A N 2001 *Phys. Rev.* E **63** 066607
[124] Serga A A, Demokritov S O, Hillebrands B, Min S and Slavin A N 2003 *J. Appl. Phys.* **93** 8585
[125] Demokritov S O, Serga A A, Demidov V E, Hillebrands B, Kalinikos B A and Kostylev M P 2003 *Nature* **426** 159
[126] Serga A A, Kostylev M P, Kalinikos B A, Demokritov S O, Hillebrands B and Benner H 2003 *JETP Lett.* **77** 300
[127] Serga A A, Kostylev M P, Kalinikos B A, Demokritov S O, Hillebrands B and Benner H 2006 *JETP* **102** 497
[128] Kalinikos B A, Kovshikov N G and Slavin A N 1983 *Sov. Phys.—JETP Lett.* **38** 413
[129] Slavin A N, Kalinikos B A and Kovshikov N G, Spin wave envelope solitons in magnetic films (chapter in [22])
[130] Bauer M, Buettner O, Demokritov S O, Hillebrands B, Grimalsky V, Rapoport Yu and Slavin A N 1998 *Phys. Rev. Lett.* **81** 3769
[131] Serga A A, Demokritov S O, Hillebrands B and Slavin A N 2004 *Phys. Rev. Lett.* **92** 117203
[132] Melkov G A, Kobljanskyj Yu V, Serga A A, Tiberkevich V S and Slavin A N 2002 *Phys. Status Solidi* A **189** 1007
[133] Melkov G A, Oliynyk A N, Serga A A, Tiberkevich V S and Slavin A N 2000 *J. Signal Process* **4** 201
[134] Melkov G A, Serga A A, Tiberkevich V S, Oliynyk A N and Slavin A N 2000 *Phys. Rev. Lett.* **84** 3438
[135] Melkov G A, Oliynyk A N, Serga A A, Slavin A N and Tiberkevich V S 2001 *Mater. Sci. Forum* **376** 785
[136] Grimalsky V V, Mantha J H, Rapoport Yu G, Slavin A N and Zaspel C E 2001 *Mater. Sci. Forum* **373–376** 377–80
[137] Zel'dovich B Ya, Pilipetskii R F and Shkunov V V 1985 *Principles of Phase Conjugation* (Berlin: Springer)
[138] Serga A A, Hillebrands B, Demokritov S O, Slavin A N, Wierzbicki P, Vasyuchka V I, Dzyapko O and Chumak A V 2005 *Phys. Rev. Lett.* **94** 167202
[139] Melkov G A, Vasyuchka V I, Chumak A V, Tiberkevich V S and Slavin A N 2006 *J. Appl. Phys.* **99** 08P513
[140] Melkov G A, Vasyuchka V I, Chumak A V and Slavin A N 2006 *J. Magn. Magn. Mater.* **300** e41
[141] Korpel A and Chatterjee M 1981 *Proc. IEEE* **69** 1539
[142] Kaplan D E 1965 *Phys. Rev. Lett.* **14** 254
[143] Kaplan D E, Hill R M and Hermann G F 1969 *J. Appl. Phys.* **40** 1164
[144] Danilov V V, Tychinskii A V and Sugakov V I 1973 *Russ. Phys. J.* **16** 316
[145] Hermann G F, Kaplan D E and Hill R M 1969 *Phys. Rev.* **181** 829
[146] How H and Vittoria C 1991 *Phys. Rev. Lett.* **66** 1626
[147] Serga A A and Tychinskiy A V 1994 *JETP Lett.* **59** 437
[148] Melkov G A and Serga A A 1988 ed Baryakthar V G and Wigen P E *Frontiers in Magnetism of Reduced Dimension Systems* (*NATO ASI Series, 3: High Technology* vol 49) (Dordrecht: Kluwer)
[149] Melkov G A, Dzyapko A D, Chumak A V and Slavin A N 2004 *JETP* **99** 1193
[150] Sparks M 1964 *Ferromagnetic Relaxation Theory* (New York: McGraw-Hill)
[151] Kobljanskyj Yu V, Melkov G A, Tiberkevich V S, Vasyuchka V I and Slavin A N 2003 *J. Appl. Phys.* **93** 8594
[152] Melkov G A, Kobljanskyj Yu V, Vasyuchka V I, Chumak A V and Slavin A N 2004 *IEEE Trans. Magn.* **40** 2814
[153] Melkov G A, Vasyuchka V I, Kobljanskyj Yu V and Slavin A N 2004 *Phys. Rev.* B **70** 224407
[154] Melkov G A, Vasyuchka V I, Chumak A V and Slavin A N 2005 *J. Appl. Phys.* **98** 074908
[155] Smith K R, Vasyuchka V I, Wu M, Melkov G A and Patton C E 2007 *Phys. Rev.* B **76** 054412
[156] Melkov G A, Kobljanskyj Yu V, Serga A A, Slavin A N and Tiberkevich V S 2001 *Phys. Rev. Lett.* **86** 4918
[157] Kobljanskyj Yu V, Melkov G A, Tiberkevich V S, Chumak A V, Vasyuchka V I and Slavin A N 2004 *J. Magn. Magn. Mater.* **272–276** 991
[158] Serga A A, Chumak A V, Andre A, Melkov G A, Slavin A N, Demokritov S O and Hillebrands B 2007 *Phys. Rev. Lett.* **99** 227202
[159] Chumak A V, Serga A A, Melkov G A, Tiberkevich V, Slavin A N and Hillebrands B 2009 *Phys. Rev.* B **79** 014405
[160] Schäfer S, Chumak A V, Serga A A, Melkov G A and Hillebrands B 2008 *Appl. Phys. Lett.* **92** 162514